



# Extreme weather anomalies and surface signatures associated with merged Atlantic-African jets during winter

Sohan Suresan<sup>1</sup>, Nili Harnik<sup>1</sup>, and Rodrigo Caballero<sup>2</sup>

<sup>1</sup>Department of Geophysics, Tel Aviv University, Israel

<sup>2</sup>Department of Meteorology, Stockholm University, Sweden

**Correspondence:** Sohan Suresan (sohansuresan@mail.tau.ac.il)

**Abstract.** The winter-long merging of the African and Atlantic jets is associated with extreme winter weather across the Northern hemisphere. Past studies have shown that merging of the Atlantic and African jets is linked to weaker Atlantic eddy activity and stronger tropical heating, and is strongly correlated with a negative NAO state. In this study we examine the relation between jet merging and extreme weather, taking care to separate out the effects of the NAO and El Niño, in order to be left with the added influence of Atlantic-African jet merging. Our analysis, considering percentile exceedance and anomaly composites of surface temperature, surface wind and precipitation, identifies distinct weather signatures of merged jet winters, notably affecting the Iberian Peninsula, North Africa, southern Mediterranean, southwest Greenland, and Northern Europe. Additionally, we analyse the relationship between merged jets and shifts in cyclone track orientation contributing to the observed extreme weather patterns over these regions. Furthermore, once we remove the NAO effect from the merged-jet surface temperature anomaly signal, we find that winter-long jet merging coincides with anomalous warm Arctic, cold Eurasia, and strong El Niño conditions. This weakens the high latitude temperature gradient which affects the midlatitude baroclinicity resulting in the weakening of eddy activity and ultimately leading to persistent jet merging. Thus the African and Atlantic jet merging during winter appears to further align with the theoretical concept that includes a dynamical regime transition of the jet from eddy driven to mixed eddy–thermally driven, consistent with the corresponding weakened mid-latitude eddies and intensified tropical heating.

## 1 Introduction

The jet stream, which appears as a relatively narrow band of local maximum of high-speed wind with large amplitude meanders in the upper troposphere, forms an important feature of the mean flow in the atmosphere. The variability in latitude, shape, and strength of the jet streams have a significant influence on our weather and climate, and could potentially increase the likelihood of a range of extreme weather events, such as cold spells, heatwaves, storms, and heavy precipitation (Screen and Simmonds, 2014). Several such extreme weather events attributed to the jet stream variability have been observed in recent decades, for example, the extreme cold winter over Europe linked to the equatorward shift of the jet during 2009-10 (Cattiaux et al., 2010; Harnik et al., 2014), the hot summer over Europe associated with a poleward jet shift in 2018 (Drouard et al., 2019), and the



extended California drought during 2011–14, associated to the wavy nature of the jet (Seager et al., 2015). Hence studies on  
25 jet streams are vital for advancing our understanding of Earth’s atmospheric dynamics and improving weather forecasts.

According to current understanding, two types of jet streams can be distinguished, based on latitudinal position and driving  
mechanism: the subtropical jets and the midlatitude jets (sometimes referred to as polar front jets). The subtropical jet (STJ),  
also referred to as “thermally driven jet”, is primarily driven by the advection of absolute angular momentum by the mean  
meridional circulation (MMC) influenced by thermal processes over the tropics and it is concentrated around the subtropical  
30 boundary of the Hadley cell (Schneider, 1977; Held and Hou, 1980). The midlatitude jet is correlated to the midlatitude  
cyclone tracks and is located inside the Ferrel cell where the eddy momentum flux convergence (EMFC) is strongest. The  
eddy momentum flux convergence by baroclinic waves is the major driving force of this “eddy-driven jet (EDJ)” (Held, 1975;  
Rhines, 1975; Panetta, 1993). There are a number of numerical studies that show the merging of these two jets and also a  
shift between single-jet and double-jet regimes due to variation in external thermal forcing and the midlatitude baroclinicity  
35 (Lee and Kim, 2003; Kim and Lee, 2004; Son and Lee, 2005; Eichelberger and Hartmann, 2007; Lu et al., 2010; O’Rourke  
and Vallis, 2013; Michel and Rivière, 2014). This theoretical evidence shows that changes in external conditions can lead to  
significant changes in the dynamical properties of the flow, resulting in a dynamical regime transition. Given a warmer future  
climate scenario, such transition could potentially occur more frequently in response to stronger thermal driving (Son and Lee,  
2005, 2006).

40 One such transition appears to have taken place throughout the winter of 2009–2010 (hereafter referred to as the 2010 winter).  
Usually, the Atlantic jet is eddy-driven and tilted meridionally, while the African jet is more of a classic STJ. The two are  
climatologically separate, with a double-jet region in the eastern Atlantic basin. However during the 2010 winter the Atlantic  
jet was exceptionally equatorward and merged with the African jet downstream into one zonally oriented jet with a structure  
and variability similar to the characteristic of the Pacific jet (Harnik et al., 2014). Using reanalysis data Li and Wettstein (2012)  
45 showed that the Atlantic jet is mostly eddy driven, whereas the Pacific jet is both thermally and eddy driven. Consequently,  
it leads to the notion that the Atlantic jet appears to have undergone a transition from being a predominantly eddy-driven to  
being a mixed eddy–thermally driven jet during 2010 winter (Harnik et al., 2014; Lachmy and Harnik, 2016). Later studies by  
Lachmy and Harnik (2020) using an idealised two-layer model have also shown that the negative phase of the annular mode of  
eddy-driven jet regimes is similar to a merged-jet regime.

50 What makes this specific 2010 winter event more interesting is that even though it has been shown that the eddy-driven jet can  
exhibit persistent southward shifts within its expected range of variability, this typically only occurs on a synoptic timescale  
(Lorenz and Hartmann, 2003; Eichelberger and Hartmann, 2007; Barnes and Hartmann, 2010). However, in this case, an  
equatorward-shifted, zonally-oriented jet configuration was persistent over an entire season and even reemerged the following  
winter. Such configuration is rare as it has only been observed once before, about 40 years prior to 2009-10, during the 1968-69  
55 winter, and is also suggestive of a dynamical jet regime transition.

It is to be noted that the 2010 winter was itself an interesting season as there were quite a few notable atmospheric and oceanic anomalies like the intense and prolonged negative phase of the North Atlantic Oscillation (NAO), a positive El Niño–Southern Oscillation (ENSO) phase and unusually cold and extreme wet weather conditions over the Northern Hemisphere (Barnes and Hartmann, 2010; Wang et al., 2010; Seager et al., 2010; Cattiaux et al., 2010; Vicente-Serrano et al., 2011; Moore and Renfrew, 2012; Santos et al., 2013). The abnormally high snowfall experienced during this winter in the mid-Atlantic states of the U.S. and northwest Europe were suggested to be primarily influenced by the negative NAO and, to a lesser extent, by the added presence of El Niño (Seager et al., 2010). In fact, the El Niño stood out as the most intense since the winter of 1997–1998 and ranked as the fifth most intense event since 1950 (National Climatic Data Center; “2009–2010 Cold Season”; 2010; NOAA’s National Climatic Data Center, Asheville, NC).

In general, the positive (negative) phase of the NAO is typically linked to relatively warm (cold) temperatures over the Europe (Hurrell, 1995). In fact, the frequency of cold event occurrence over the extratropical Northern Hemisphere during winter and warm extremes over North Africa and Arab regions are strongly influenced by the NAO (Thompson and Wallace, 2001; Donat et al., 2014). Meanwhile, ENSO is also known to affect both mean and extreme precipitation and temperature levels in many parts of the Northern hemisphere (Ropelewski and Halpert, 1986; Schubert et al., 2008; Alexander et al., 2009; Kenyon and Hegerl, 2010; Arblaster and Alexander, 2012; Donat et al., 2014). It is even shown using dynamic models that the exceptionally severe winters in Europe during 1940–1942 were influenced by the propagation of ENSO signals from the troposphere to the stratosphere, impacting the phases of the Arctic Oscillation (AO) (Brönnimann et al., 2004). Although the variability in winter climate across much of the Northern Hemisphere is prominently influenced by the NAO and the ENSO phases (Hurrell, 1995; Brönnimann et al., 2004), the added influence of jet merging on such extreme weather patterns remains unexplored.

In this study, we investigate the influence of prolonged jet merging over a month or longer on weather extremes, and examine how this effect differs, if at all, from the impact of a strongly negative NAO and El Niño. We aim to understand whether the extreme weather patterns observed during jet-merging winters result solely from the combined influence of NAO and El Niño, or if there is an additional impact from the merged jet across the Atlantic specific to these months. Our analysis seeks to uncover unique signals associated with the possible dynamic regime shift of Atlantic–African merged jet winters, particularly in relation to extreme surface temperature, surface wind, and precipitation distributions across the Northern Hemisphere.

## 2 Data and Analysis methods

The analyses carried out in this study are all based on the daily/monthly-averaged December–February (DJF) data of wind, precipitation, and temperature, from the ERA5 reanalysis (Hersbach et al., 2023a) of the European Centre for Medium-Range Weather Forecasts (ECMWF) at a spatial resolution of  $0.25 \times 0.25$  from January 1950 to December 2020. We used the National Oceanic and Atmospheric Administration (NOAA) Climate Prediction Center (CPC) NAO index (based on Jianping and Wang (2003)) and Oceanic Niño Index (ONI) derived from the ERSST v5 analysis [Huang et al., 2017].



The Zonal Jet Index (ZJI), which is adapted from Harnik et al. (2014), helps us to identify merged-jet time periods. In order to calculate the ZJI, we use the zonal wind:  $u_{300}[\lambda, \phi, t]$  at 300hPa. We first find the latitude of the jet axis  $\hat{\phi}(\lambda)$ , defined at each longitude  $\lambda$  as the latitude  $\phi$  with maximum magnitude of  $u_{300}$ , and calculate the maximum absolute value of its zonal derivative  $|\frac{d\hat{\phi}(\lambda)}{d\lambda}|$ . This term will have the largest magnitude at the point where the jet axis jumps from the Atlantic to the African jet. Zonal Jet Index (ZJI) is defined by taking the absolute value of this maximum latitude change over longitude  $[\max(|\frac{d\hat{\phi}(\lambda)}{d\lambda}|)]$ , and calculating its monthly anomaly from the climatological seasonal cycle. During jet mergings the zonal jump in jet axis latitude will disappear, hence the ZJI will have large negative values.

To study the variability in the distribution of extreme winter weather during merged-jet events we first classify the winter months (December-February) into 5 groups as follows:

- (a) Winter months with strong Atlantic-African merged jet state: lower than -2 times standard deviation of winter monthly ZJI. (14 winter months)
- (b) Winter months with strong negative NAO phase: monthly NAO index lesser than -1 times of its standard deviation. (29 winter months)
- (c) Winter months with strong negative NAO phase: monthly NAO index lesser than -1 times of its standard deviation, but excluding strong negative ZJI months in group (a). (20 winter months)
- (d) Winter months with strong El-Nino phase: monthly ONI value larger than 1. (32 winter months)
- (e) Winter months with strong El-Nino phase: monthly ONI value larger than 1, but excluding strong negative ZJI months in group (a). (25 winter months)

For the time period to be consistent we select winter months from a period of 1959-2020 as the cyclone tracks data used for analysis are available only over this time period. The detailed table of the exact winter months in each group and their overlapping months are shown in the supplementary information (Table S1 and S2). From Table S2, we see that all the merged-jet (-ZJI) winter months except one have a -NAO phase, and most of these -ZJI months coincide with a strong -NAO or El Nino phase or even both.

We then examine the daily-mean data to identify the regions of extreme weather within each group mentioned above. We first calculate the 95th and 5th percentiles of daily 2m temperature, 10m wind, and daily precipitation, for each grid point, with the percentiles calculated based on all winter days in the data set. We then count the number of winter days within our different winter groups, that exceed these thresholds (say warmer than the 95th, or colder than the 5th percentiles). Regions where these thresholds are exceeded for 10 percent or more of the time, are then recognized as areas for which the relevant winter group tends to increase the likelihood of the extreme weather type examined. For example, locations where the 95th percentile temperature was exceeded more than 10% of the time imply an enhancement of warm extremes, while regions where the temperatures are colder than the 5th percentile for 10% or more of the total winter days imply an enhancement of cold extremes. Correspondingly, we also identify regions for which extremes are less likely to happen as those for which the



120 thresholds were exceeded less than 1 percent of the total winter days. The regions of statistical significance for these percentage of winter days are calculated using the Monte Carlo significance test.

To study the added influence of merged-jet winter signals on a monthly scale, ENSO and NAO signals are removed from monthly anomaly composites by linearly regressing out ONI and NAO indices before conducting the analysis. This methodology is used in many previous studies (Kim et al., 2023; Chang et al., 2007; Zhang et al., 2014; You and Furtado, 2017; Amaya, 2019). To investigate the impact and significance of synoptic scale eddies, we split the primary daily-mean datasets into shorter and longer time scales using a basic boxcar filter with 10 days cutoff. This allows us to define eddies as the data filtered with a 10-day high-pass filter, while the mean flow corresponds to the data filtered with a 10-day low-pass filter. Subsequently, we compute eddy fluxes by assessing the low-pass covariances between the high-pass fields. For identifying and comparing cyclone density we use cyclone track data based on the extratropical cyclone tracks over the Northern Hemisphere, produced by applying a cyclone tracking algorithm (Murray and Simmonds, 1991; Pinto et al., 2005) on the ECMWF ERA5 reanalysis mean sea level pressure data (remapped to 1.125 lat-lon degrees). The algorithm is run for the Northern Hemisphere region 20°N–90°N from a time period of 1959 to 2021 at a 6-hr time interval. Detailed information about the methodology can be found in (Murray and Simmonds, 1991; Pinto et al., 2005, 2009). It is worth noting that cyclone tracks based on (Pinto et al., 2005) are recognized for being often longer in terms of both lifetime and track, compared to those derived from alternative tracking methods (see Neu et al. (2013)).

### 135 3 Extreme weather distribution during merged-jet winter

As extreme weather events have been observed in connection with merged jet (-ZJI), negative NAO (-NAO), and El Niño winters, our initial investigation focuses on the frequency of days with extreme weather across the Northern Hemisphere during the entire winter period. In this section, we examine the distribution of 2m surface temperature, 10m surface wind, and precipitation across -ZJI, -NAO and El Niño winter months.

#### 140 3.1 Surface Temperature

Figure 1 shows the distribution of the percentage of days that experience warm extremes (exceeds the 95 percentile of 2m surface temperature) for each winter group described in the previous section. Here we see in Fig.1a, that the winter days with merged jet state, have a distinctive warm day distribution that is different from the others. The stippled regions in the gradient of red indicate the number of warm extreme days of 10 percent or more with a statistical significance of 99% while regions in white indicate fewer warm extreme days. There are 5 regions with increased warm extreme occurrence during merged-jet winters: Greenland, North, and South subtropical Atlantic, North Africa - Mediterranean, and central Pacific. Looking at NAO with and without -ZJI months (Fig.1b-c) and ENSO with and without -ZJI months (Fig.1d-e) we see that the tropical Pacific and southern subtropical Atlantic appear in the ENSO months, both with and without the -ZJI, suggesting they are an ENSO signal, while Greenland appears in the -NAO months, though to a lesser extent when -ZJI months are removed, suggesting this is partly a negative NAO signal, but the jet merging extends the number of extreme warm days over Greenland significantly. The warm



extreme over subtropical North Atlantic and North Africa-Mediterranean appears dominant in the -ZJI months, suggesting they are associated with the jet merging. We also see 2 regions of low warm extreme days - Europe and the southeastern tropical Pacific. The tropical eastern Pacific region appears in the -NAO months, with and without -ZJI, indicating this is due to -NAO. Note that the -NAO and El Niño signals oppose each other during the -ZJI months with the NAO signal dominating in the eastern tropical Pacific with anomalously few extreme warm days and El Niño dominates in the central tropical Pacific with more extreme warm days. The reduction of extreme warm days over Europe, however, only appears predominantly in the -ZJI groups, suggesting the stronger correlation of anomalous jet merging to less extreme warm days over Europe.

To have a better understanding of the daily surface temperature distribution for each winter, we examine box plots for specific regions of interest highlighted in the boxes shown in Fig.1a. Figure 2a-d illustrates the box plot of area-averaged daily surface temperatures over tropical-subtropical North Atlantic, North Africa-Mediterranean, Greenland, and Europe respectively. The plots show climatology winters (1960-2020), El Niño winters (excluding -ZJI), -NAO winters (excluding -ZJI), and merged jet (-ZJI) winters. The tropical-subtropical North Atlantic region shows a shift to warmer surface temperature during merged jet months with El Niño contributing to the overall warm extremes more than -NAO. Over the North Africa-Mediterranean regions, the merging contributes to the strongest extremes and a warmer region in the mean. In Greenland jet merging contributes to many of the extremes including the most extreme warm days, as well as to the mean while in Europe clearly there are less warm extremes and the mean temperature during jet merging is lower than during ENSO and -NAO winters. We also note that in Greenland, merged jet winters have fewer cold extremes compared to other winters.

We next examine the relation between jet merging and the occurrence of extreme cold days (Fig.3a-c), by examining the number of days that are colder than the 5th percentile of temperature. Here we highlight the regions greater than the 10% threshold in gradient of dark blue - these are regions that experience a larger number of extreme cold days, and we highlighted regions in which extreme cold days occur less than 1% in white- these are regions in which the chosen months experience fewer extreme cold days. From Fig.3a we see that during -ZJI months the increased extreme cold days mostly occur in the north-western European region. This pattern forms a belt stretching from the eastern US coast, extending to the Scandinavian region, encompassing the UK and other Northern European countries, and even branching into Asia. Looking at NAO with and without -ZJI months (Fig.3b-c) we see that the cold extremes on the western-central US are influenced by -NAO whereas the eastern coast is influenced by the jet merging. The cooling over the tropical eastern Pacific region appears in the -NAO months, with and without -ZJI, indicating this is primarily associated with -NAO although the jet merging extends the number of extreme cold days slightly towards the central Pacific.

We also see that the Arctic region exhibits more pronounced cold extremes during -NAO when not accompanied by merged jet. Negative NAO tends to induce stronger cooling in high-latitude Eurasia and the Arctic. This also indicates that -ZJI winters have a warmer Arctic compared to -NAO when not accompanied by merged jet which raises the potential influence of Arctic warming on merged jet formation. We also see some regions of fewer cold extremes during jet merging - North Africa, subtropical Atlantic, western Greenland and central Pacific, which coincide with the regions of high warm extremes seen earlier during jet merging. The distribution of cold extremes across the Northern Hemisphere is observed to be notably weak

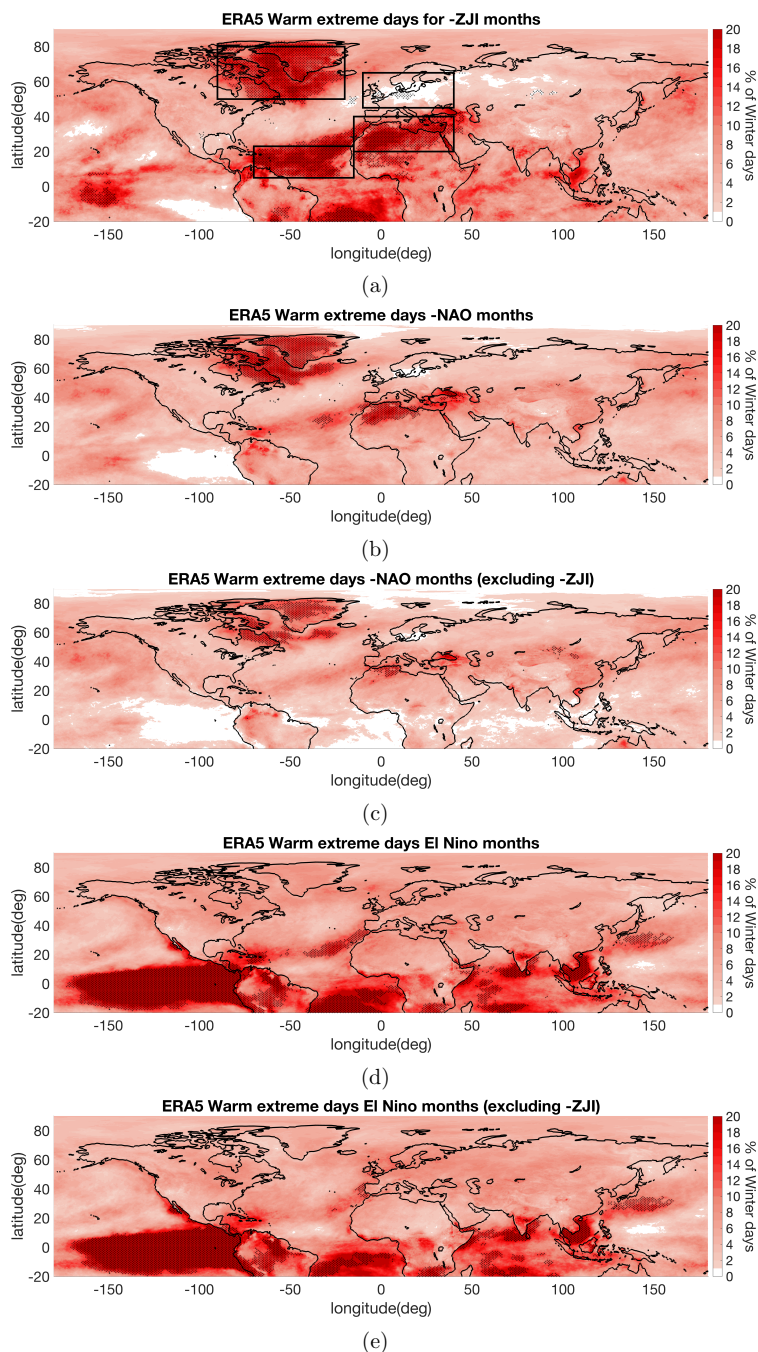


**Figure 1.** The distribution of the percentage of warm extreme days for (a) merged jet winter months (b) negative NAO winter months (c)negative NAO winter months excluding merged jet months (d) El Nino winter months (e)El Nino winter months excluding merged jet months. The regions stippled in black (+) represents regions significant at 99% using Monte Carlo simulation.

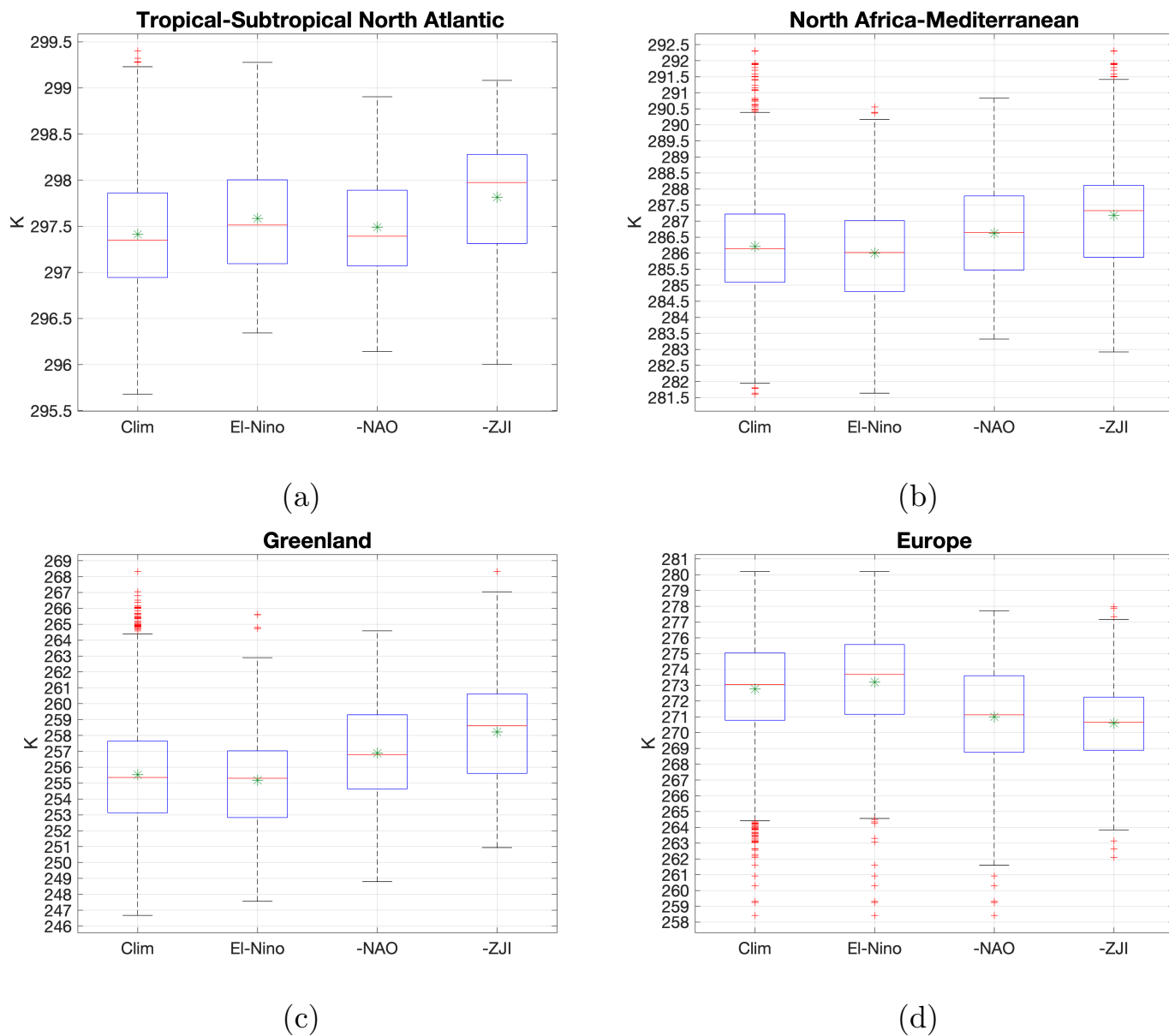


**Figure 2.** Box plot of daily average surface temperatures for DJF Climatology (1960-2020), El Niño months (excluding -ZJI), negative NAO months (excluding -ZJI) and merged jet months(-ZJI) over (a) the tropical-subtropical Atlantic within the region of [5°N-23°N,70°W-15°W],(b) the North African-Mediterranean [20°N-40°N,-15°W-40°E],(c)the Greenland region [50°N-80°N,90°W-20°W],(d)Europe [65°N-45°N,10°W-40°E]. These regions are marked in boxes in Fig.1a. In each box plot, the red line represents the median, while the lower and upper edges of the box represent the 25th and 75th percentiles, respectively. The whiskers stretch to the furthest data points that are not deemed outliers, which are values that are more than 1.5 times the interquartile range away from the bottom or top of the box, and any outliers are depicted individually with a red (+) marker symbol. The value marked in green (\*) represents the average value.



185 in terms of their influence by El Niño, both with and without the -ZJI (Fig.S1a-b shown in supplementary). The box plot over the regions of the south-eastern US and the Arctic as shown in boxes in Fig.3a are shown in Fig.3d-e. Here we see that the south-eastern US shifts to a colder surface temperature on average during merged jet, contributing to the extremes including the most extreme cold days. Whereas during jet merging the Arctic seems to have a warmer surface temperature and contributes more to the warm extreme days among the climatology while -NAO contributes more to the cold extreme days.

190 As shown in Harnik et al. (2014) (see their Fig.11), most of the -ZJI winter months coincide with either strong El Niño or negative NAO or even both. It is thus essential to explore whether the -ZJI operates independently of the influence of ENSO and NAO or is intertwined with it. In order to do so, we examine composites of monthly mean surface temperature anomalies associated with -ZJI, before and after regressing out the ENSO and NAO signals from the surface temperature detrended data field. Figure 4a shows the monthly anomaly composite of detrended surface temperature for the -ZJI winter months, where

195 we see the typical tripole pattern over the Atlantic ocean often associated with the -NAO phase and warming over tropical eastern Pacific Ocean associated with the El Niño phase. We also see anomalous warming over North Africa, Mediterranean, Greenland, and the entire tropical Atlantic while anomalous cooling over most of Eurasia and Central US. These composite anomalies are consistent with the results for temperature extremes shown in Fig.1a and Fig.2a. From this, we remove the ENSO and NAO signals using linear regression analysis resulting in Fig.4b. Upon their comparison, it is evident that the anomalous

200 temperature distribution associated with extreme weather during the -ZJI winter persists, though at a reduced magnitude, even after removing ENSO and NAO signals. Additionally, there emerges a noteworthy anomalous warming over the Arctic region. This warming trend during the -ZJI winter was previously obscured by the prevailing NAO and ENSO signals, particularly the dominant NAO signal in the Arctic, as evidenced by individual signal removal analyses (see Fig.S2a-b in supplementary materials). Such an anomalous warming trend is known to affect midlatitude baroclinity and weaken the eddy fluxes over these

205 regions (Yuval and Kaspi, 2020; Chemke and Polvani, 2020). Hence this anomalous warmer Arctic and colder Eurasia could explain the weakened eddy activity over the midlatitude during -ZJI winters as observed during 2010 winter (e.g. Harnik et al., 2014, see their Fig.6). Combine this with the coinciding stronger tropical forcing, a merged Atlantic-African jet indeed draws a real world picture of the external forcing pushing the large scale flow dynamical regime from an eddy-driven jet state towards a merged jet state, as shown using idealised models in previous studies such as Son and Lee (2005) and Lachmy and Harnik

210 (2014, 2016). Furthermore, the warmer Arctic could be associated with the Arctic Amplification (AA) and Arctic sea-ice loss, as several theories posit its role in modulating meridional circulation patterns by affecting midlatitude baroclinicity thereby impacting the occurrence of extreme winter weather across the midlatitudes (Francis and Vavrus, 2012; Kim et al., 2014; Peings et al., 2023; Cohen et al., 2014, 2021; Kinnard et al., 2011; Rantanen et al., 2022). Given that the Arctic is warming faster than higher latitudes, and the tendency for more extreme El Niños to happen in the future (Cai et al., 2014; Wang et al., 2019), these

215 findings suggests that such winter-long jet merging can occur more frequently under global warming scenarios in the future thus motivating further investigation.

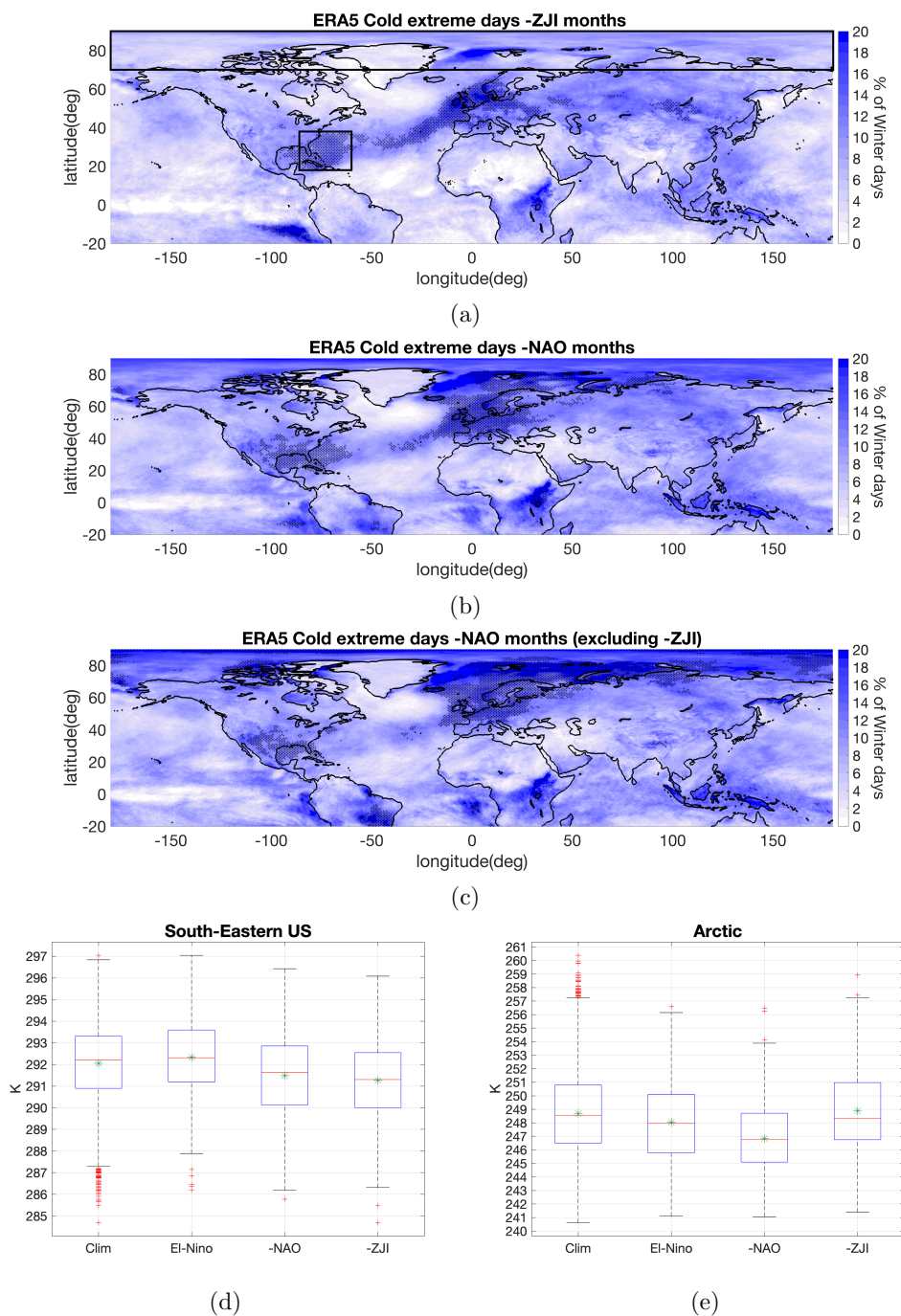


**Figure 3.** The distribution of the percentage of cold extreme days for (a) merged jet winter months (b) negative NAO winter months (c)negative NAO winter months excluding merged jet months. The regions stippled in black (+) represent regions significant at 99% using Monte Carlo simulation. Box plot of daily average surface temperature similar to Fig.2 over (d) south-east US coast [18°N-38°N,86°W-60°W] and (e)Arctics [70°N-90°N,180°W-180°E].These regions are marked in boxes in Fig.3a

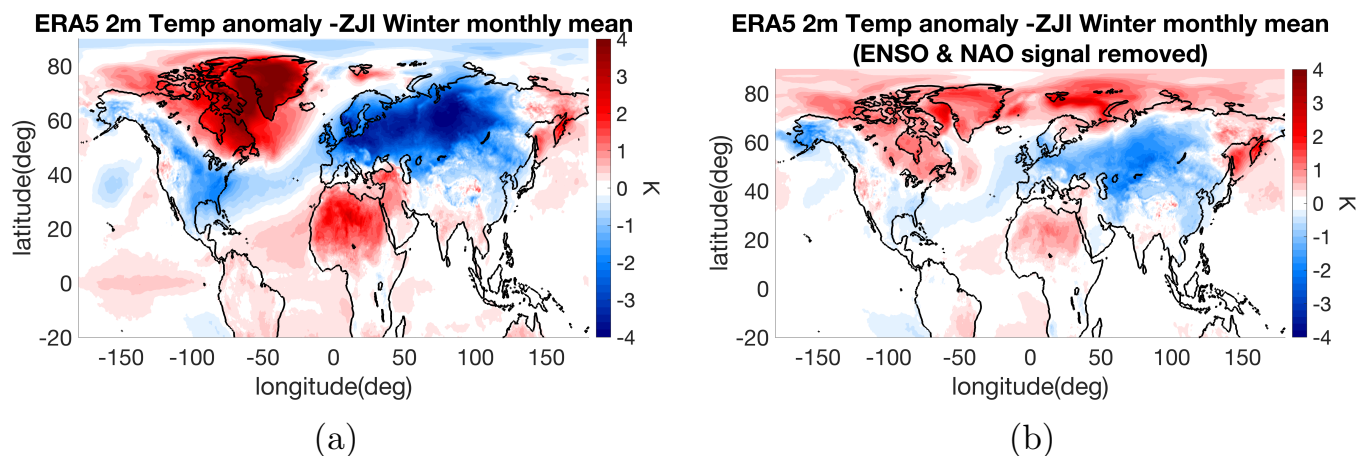


**Figure 4.** (a) Composite for anomalous detrended 2m surface temperature (K) for -ZJI winter months. (b) Same as (a) but removed the NAO and ENSO signals using linear regression analysis.

### 3.2 Surface Wind

Now we analyse the surface wind extremes, similar to the previous section, by examining the percentage of days within each winter group that experiences extreme strong wind (surpass the daily 95th percentile 10m surface wind) with respect to climatology. In Fig.5a, we observe that extreme surface winds during -ZJI winters are primarily concentrated over the subtropical Atlantic, Greenland, and the Eastern tropical Pacific in the southern hemisphere. The wind extremes over the subtropical Atlantic align with the equatorward-shifted, zonally-oriented jet. Additionally, there are strong winds throughout the Greenland region. A comparison with Fig.5b reveals that similar strong winds occur during -NAO winters, excluding -ZJI winters, over these regions with the distinction that the frequency of such days is higher during merged jet winters. Notably, over the subtropical Atlantic, the wind extremes are predominantly situated in the east during -NAO winters, contrasting the more evenly distributed pattern observed during jet merging. The most notable contrast in the distribution of extreme winds between -ZJI winter and -NAO winter is observed over the Eastern tropical Pacific in the southern hemisphere, as highlighted in the box in Fig.5a. In this region, there is a discernible increase in the frequency of extreme strong surface winds during -ZJI winter, a pattern not evident in -NAO winters. This difference is partly attributed to the influence of El Niño, as similar analyses for El Niño winters show a much weaker but comparable pattern (refer to Fig.S3b-c supplementary for details).

The box plots of area-averaged daily mean surface wind over Greenland and the Eastern tropical Pacific region, marked in boxes in Fig.5a, are shown in Fig.5c-d respectively. Over Greenland, there appears to be stronger wind during merged jet months with -NAO also contributing to the extremes. Except for one very weak wind day the jet merging contributes mostly to the strongest wind days and to the mean. Over the Eastern tropical Pacific, both the mean and median surface wind during -ZJI winter days surpasses those observed in -NAO (excluding -ZJI), El Niño (excluding -ZJI), and climatology winter days. This shift signifies a higher concentration of strong winds over this region during -ZJI winter days. Previous study by Harnik et al.

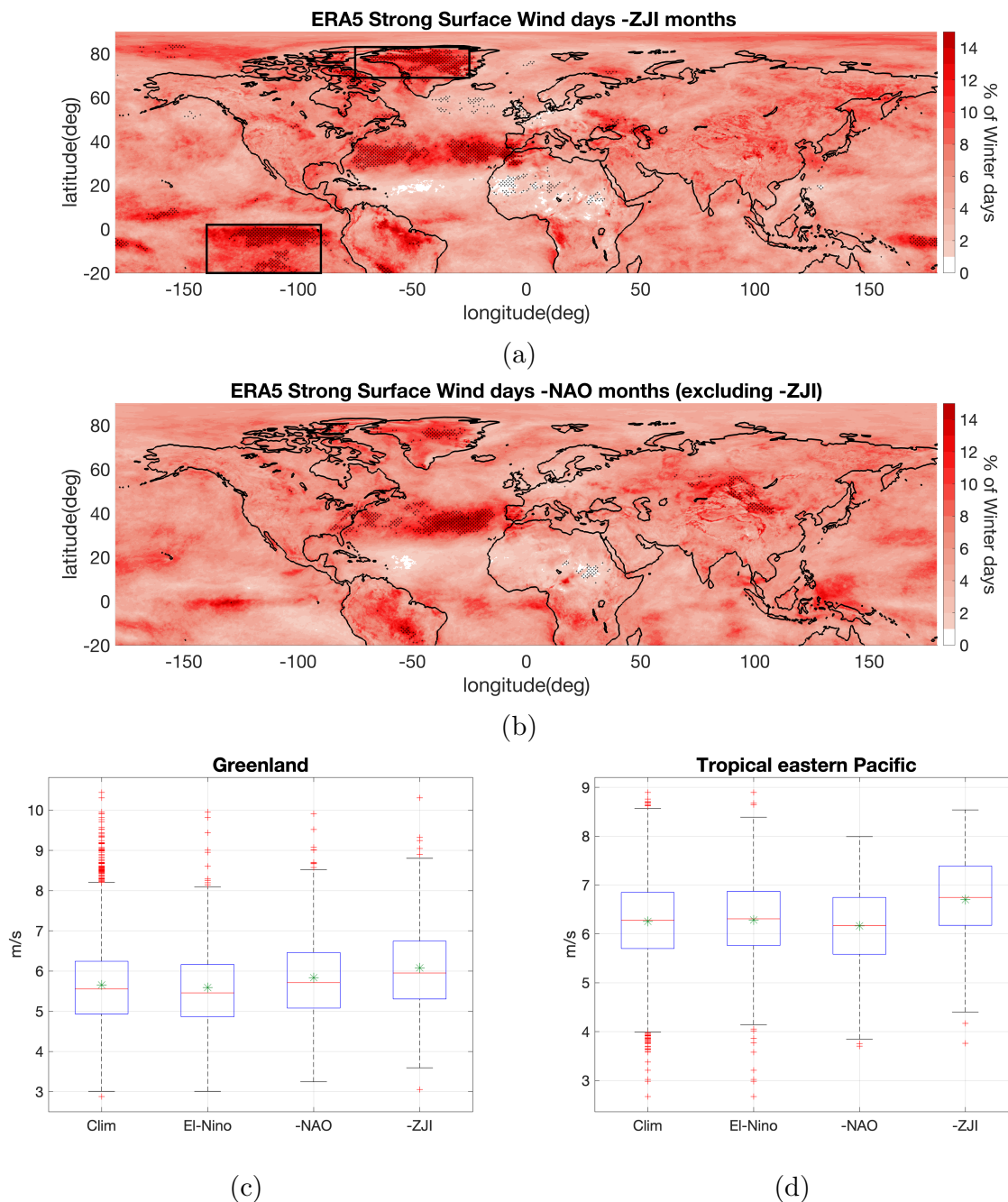


**Figure 5.** The distribution of the percentage of strong surface wind days for (a) merged jet winter months (b) negative NAO winter months excluding merged jet months, the regions stippled in black (+) represents regions significant at 99% using Monte Carlo simulation. Box plot, similar to Fig.2, of daily wind averaged over (c) Greenland [69°N-83°N,75°W-25°W] (d) tropical eastern-pacific [20°S-2°N,140°W-90°W]. These regions are marked in boxes in Fig.5a

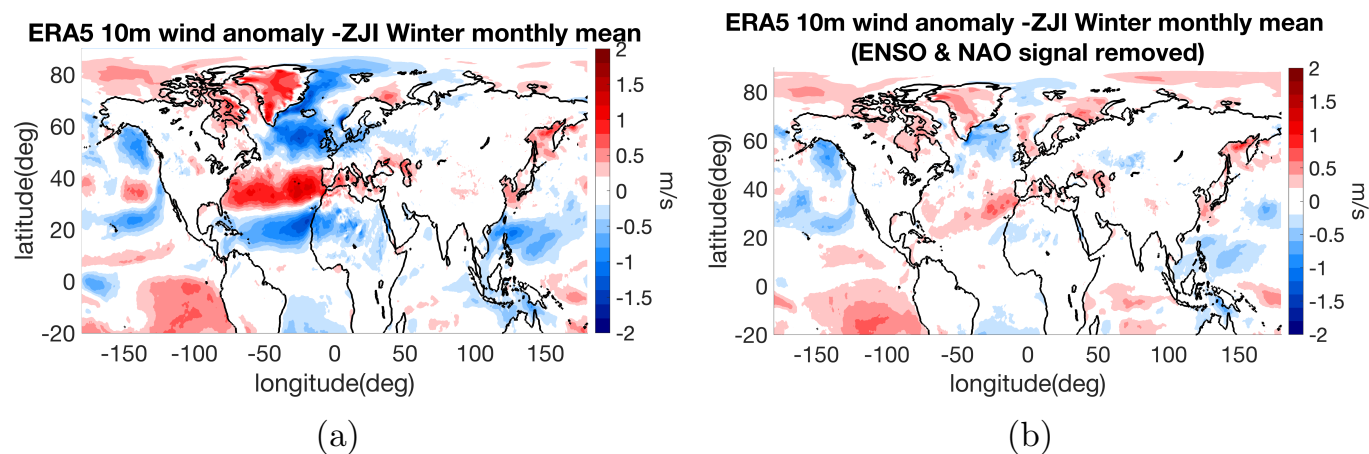


**Figure 6.** (a) Composite for anomalous 10m surface wind (m/s) for -ZJI winter months. (b) Same as (a) but removed the NAO and ENSO signals using linear regression analysis.

(2014), employing back-trajectory analysis of the Atlantic subtropical jet, demonstrated a significant northward displacement of air parcels from the equatorial eastern tropical Pacific region to the subtropics. This displacement can contribute to the Atlantic jet, establishing the tropical Pacific as one of the sources of momentum for the formation of the merged jet. At the same time, the observed higher concentration of strong winds over the Eastern tropical Pacific during -ZJI winter months could also be influenced by increased storm activity over the region during jet-merging, necessitating further analysis to validate these findings.

Now we examine the 10m surface wind anomaly composite for -ZJI winter months as shown in Fig.6a. Here we see the presence of strong wind over the subtropical Atlantic Ocean aligning with the zonally oriented merged jet with weaker winds on either side: towards the midlatitude and tropics. We also see the strong wind at the tropical eastern Pacific and over polar region near Greenland. This coincides with the regions experiencing the extreme wind during the -ZJI winter shown in Fig.5a. From this, we remove the NAO and ENSO signal resulting in the residual wind signals, shown in Fig.6b. This plot shows that the stronger surface wind contributed from the merged jet event over the Atlantic, forms a belt stretching from the coast of Cuba extending north-east with stronger wind towards the Iberian Peninsula. This explains the fewer surface wind extremes towards the west of Atlantic during -NAO winter without -ZJI shown in Fig.5b. We also see that the strong wind activity over the tropical eastern Pacific continues to exist even after removing the NAO and ENSO signal. This may indicate an anomalous overturning circulation that gives rise to the ongoing air flows into the Atlantic jet from the subtropical Pacific (as implied using lagrangian air parcel trajectories in Harnik et al. (2014)), but further study of the nature of the extreme surface wind anomalies is needed to determine the robustness and physical phenomena behind this signal. Additionally, we observe the strong wind anomaly persisting over the polar region near Greenland which could be the result of potential shift in cyclone tracks to Greenland and the Arctic Archipelago during -ZJI winter months.



### 3.3 Precipitation

Similar to the previous analysis, we now examine the total precipitation. Figure 7a shows the frequency of days with high precipitation (exceeding the 95th percentile daily precipitation) for -ZJI winter. Here we see that the extreme high precipitation is concentrated over the Iberian Peninsula and the western Greenland region. The former is consistent with the previous study (Vicente-Serrano et al., 2011) which showed the prolonged occurrence of rainy days during the winter of 2009/2010, exhibiting an unusually high frequency across much of the Iberian Peninsula. The study delves into the notable influence of the extreme negative winter NAO on precipitation in the western and southern areas of Iberia. Additionally, it highlights the potential correlation between the southward displacement of the jet during the winter of 2010 and the anomalously intense precipitation, distinguishing it from other winters characterized by a strongly negative NAO. This correlation is clearly evident when comparing Fig.7a and Fig.7b where we see a higher frequency of extreme precipitation during -ZJI winter compared to -NAO winter (excluding -ZJI) over regions of Iberian Peninsula and Northern Africa and regions over western Greenland. We also looked into similar plot for El Niño winter (see Fig.S4a-b in supplementary) but no substantial contributions were identified over these regions. Figure 7c and Fig.7d display the box plot of total daily precipitation averaged over the regions of western Greenland and the areas covering the Iberian Peninsula and Northern Africa respectively (marked in boxes in Fig.7a). In western Greenland, both the mean and median total precipitation are higher during -ZJI winter compared to -NAO (excluding -ZJI), El Niño (excluding -ZJI), and climatology winter days. Additionally, there are notable extreme daily precipitation from the climatology that fall within the -ZJI winter days. A more extreme pattern is observed over the Iberian Peninsula, where the mean total precipitation during -ZJI winter is significantly higher than the average climatology and El Niño winters, and slightly higher than -NAO winter. Furthermore, the larger daily precipitation from the climatology fall within the -ZJI winter days, indicating extreme precipitation during the merged jet winters. It is also interesting to note from Fig.7e, which shows the frequency of days with low precipitation (less than 5th percentile of daily precipitation), that the low precipitation extreme is concentrated mostly over the south of Greenland during -ZJI winter in proximity to the one of the deep-water formation regions. Jet merging appears to result in reduced precipitation input over this region south of Greenland during winter. Now for the precipitation composite anomaly for -ZJI winter month, we look into Fig.8a. We see that over the Atlantic Ocean, the precipitation anomaly is higher over the subtropics aligning with the stronger wind anomaly here during -ZJI months. We also see the stronger precipitation anomaly over the western coast of Greenland and weaker precipitation anomaly over the eastern coast. The stronger precipitation anomaly over the tropical Pacific appears due to the higher convection over this region from strong ElNiño conditions. Once we remove the NAO and ENSO signal from this the residual signal appears as shown in Fig.8b. Here we see that the precipitation anomaly over the Iberian Peninsula still persists even though the anomaly over the western Atlantic weakens, indicating the stronger precipitation over Iberian Peninsula during merged jet winter. We see a similar pattern over the western coast of Greenland while over the south-eastern Greenland coast, there is a negative precipitation anomaly signal which coincides with the region of low precipitation extreme seen earlier during jet merging. Even though we removed the ENSO signal we see a strong precipitation anomaly over the tropical eastern Pacific region and increased precipitation over

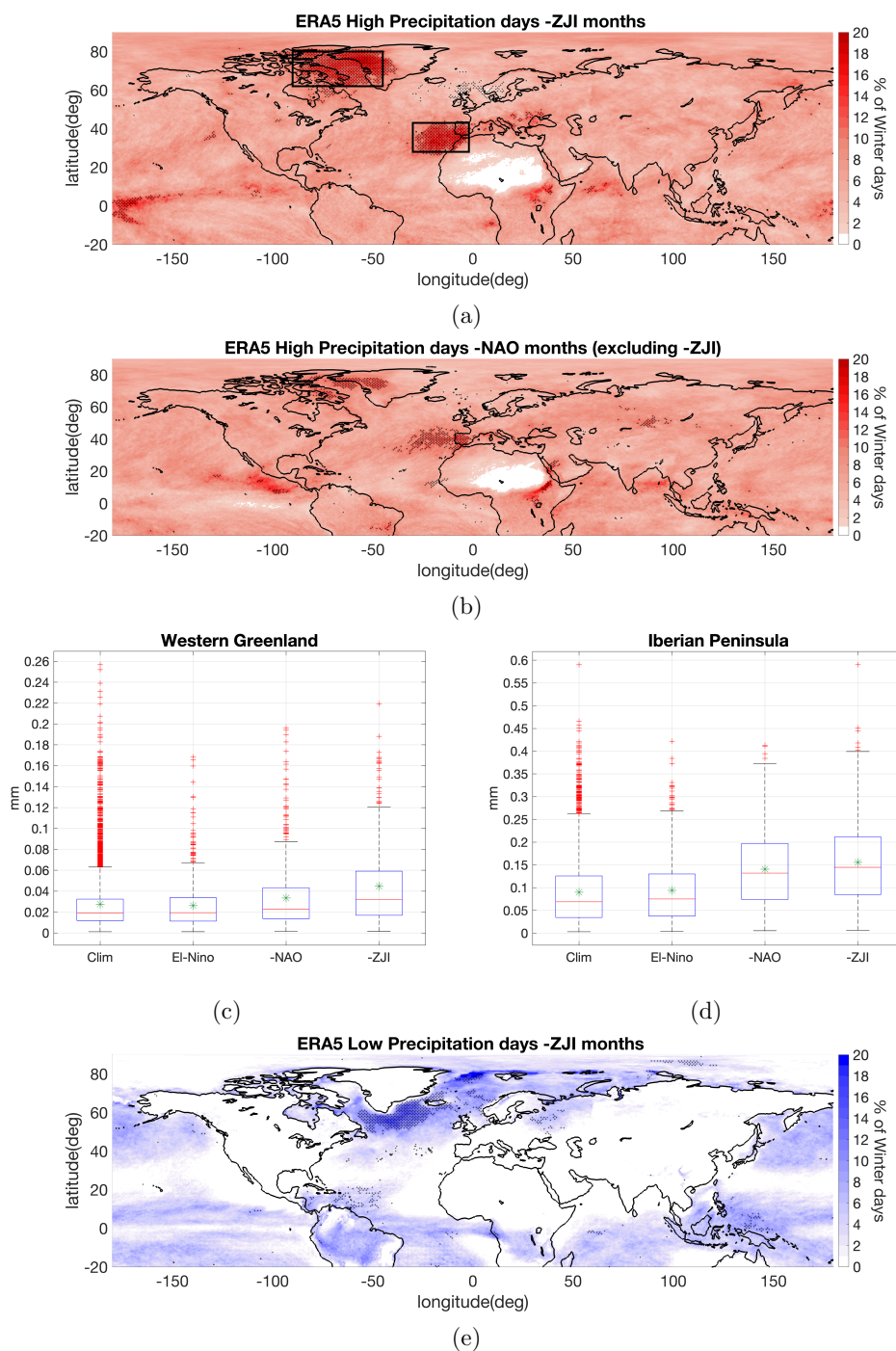


**Figure 7.** The distribution of the percentage of high precipitation days for (a) merged jet winter months (b)negative NAO winter months excluding merged jet months. Box plot, similar to Fig.2, of daily wind averaged over (c) western Greenland [62°N-80°N,90°W-45°W], (d) the Iberian Peninsula[28°N-43°N,30°W-2°W] (boxes marked in Fig.7a). The distribution of the percentage of low precipitation days for (e) merged jet winter months. The regions stippled in black (+) represent regions significant at 99% using Monte Carlo simulation.

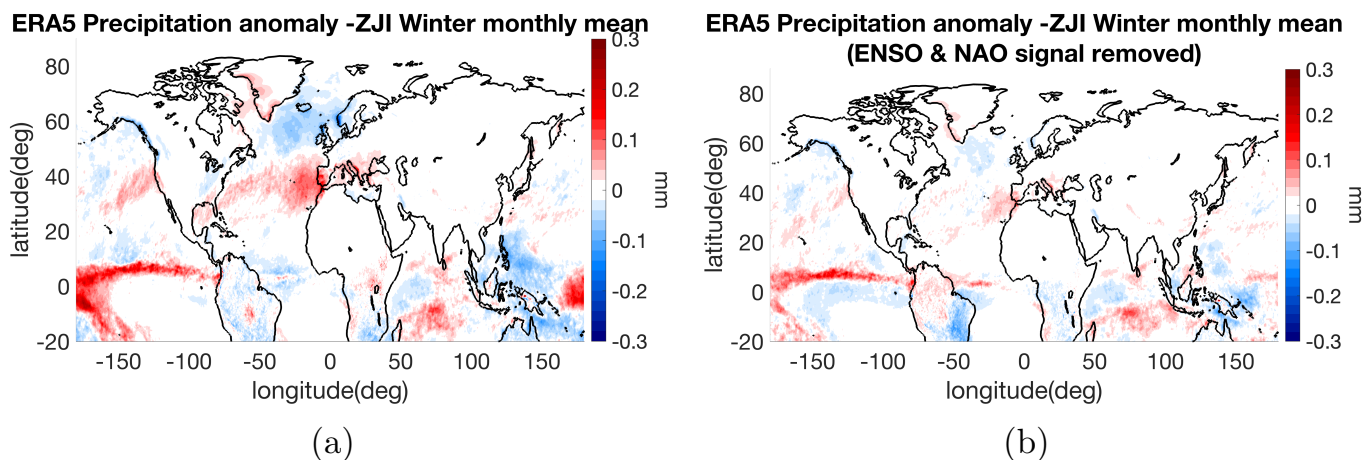


**Figure 8.** (a) Composite for anomalous total precipitation (mm) for -ZJI winter months. (b) Same as (a) but removed the NAO and ENSO signals using linear regression analysis.

290 South America. The role of wind patterns and cyclone formation during jet merging months contributing to this distribution needs to be investigated further.

#### 4 Cyclone track analysis

We know that cyclones represent rotating weather systems capable of causing substantial rainfall, heightened surface winds, and destructive surges. The jet stream plays a significant role in both the initiation and intensification of cyclones and also  
295 influences the positioning of storm tracks (Holton, 2007; Pinto et al., 2009). Therefore, it is of interest to investigate and compare the potential impact of cyclones on regional extreme weather during -ZJI winter months. Figure 9a-c shows the composite plot of the cyclone density anomaly during the -ZJI winters, -NAO winters (excluding -ZJI) and the difference between them respectively with 10m surface eddy kinetic energy (EKE) anomaly in contours. The cyclone density anomaly during the -ZJI winters shows that the cyclones have anomalously shifted southward and zonally oriented as expected due to the  
300 merged jet formation, influencing the cyclonic activity near the Iberian Peninsula, northern Africa, and much of the western and central Mediterranean. It is well known that the NAO influences the positioning and alignment of cyclone tracks, resulting in a northeastern extension of storm tracks during positive NAO phases and a southward shift during negative NAO phases (Pinto et al., 2009). This southward shift is exactly what we observe in Fig.9b for -NAO winter months, but on comparing it with Fig.9a we see that during -ZJI months the cyclone tracks are oriented even further south compared to -NAO months. It is also  
305 important to note that during -ZJI winter months, there is a higher cyclone density over the western regions of Greenland, which is not common in the usual -NAO winters. This distinction is evident from Fig.9c, where an increased concentration of cyclone is observed along the coast of Greenland and over the Atlantic at latitudes between 30°N-40°N.

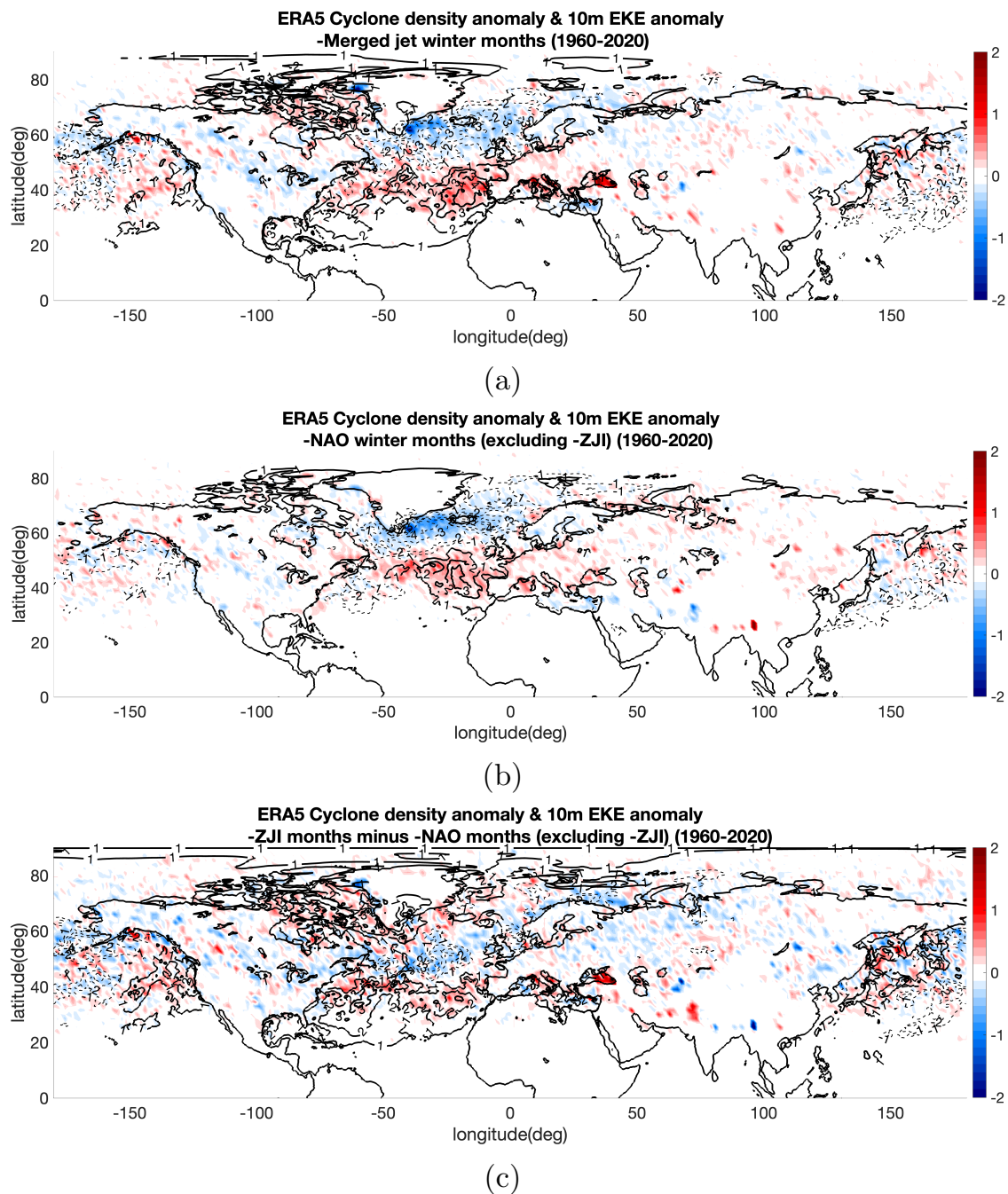


**Figure 9.** The cyclone density (number of cyclones per month per grid point) monthly anomaly composite during (a) merged jet winter (b)negative NAO winter months excluding merged jet months (c) the difference of cyclone density monthly anomaly between (a) and (b). The surface eddy-kinetic energy ( $m^2 s^{-2}$ ) anomaly is shown in contours. The positive and negative values are shown in solid and dashed lines respectively.



The increased (decreased) anomaly in cyclone track density coincides with the positive (negative) anomaly of surface EKE. While both -NAO winters and -ZJI winters exhibit weaker EKE in the midlatitude Atlantic, -ZJI winters stand out with stronger  
310 EKE, particularly over western Greenland and over the 40°N Atlantic region. This indicates that during jet merging, the usually northeast-oriented cyclone tracks over the Atlantic not only shift southward similar to -NAO winters but also extend to the western Greenland region with the stronger eddy kinetic energy. Hence following cyclogenesis at the subtropical East Atlantic, there appears to be notable deviation from the conventional northeastward trajectory of cyclones during jet merging. A significant proportion of cyclones exhibit a zonal migration towards the eastern Atlantic, extending across the Mediterranean, while  
315 certain cyclones move towards the western coast of Greenland, becoming ensnared amidst the Arctic Archipelago region. This phenomenon elucidates the aggregation of extreme anomalies observed over western Greenland, the dry weather experienced in northern Europe, and the heightened frequency of precipitation in the Iberian Peninsula, as discussed in the previous section.

## 5 Conclusions

In this study, we start by analysing how extreme weather events are distributed across the Northern Hemisphere when the  
320 Atlantic and African jets anomalously merge during winter. We explore how the distribution of surface temperature, precipitation, and surface wind differs during merged-jet winter months from those observed during typical winters influenced by strong negative NAO and El Niño conditions.

Firstly, we have identified a distinct pattern of extreme surface temperature distribution during merged jet winters, covering the Mediterranean, North Africa and the subtropical Atlantic regions forming a warm extreme belt at the lower latitudes. This warm  
325 extreme belt is much weaker and poorly distributed during a typical strong -NAO winter in the absence of merged Atlantic and African jets indicating a stronger correlation between merged jet activity and extreme temperature distribution at lower latitudes. Additionally, over the higher latitudes warmer surface temperature extremes are observed over Greenland during merged jet winters, while cold extremes predominates in northern Eurasian regions. We also looked into whether merged-jet winters operate on extreme surface temperature distribution independently of, or are intertwined with, the influences of  
330 ENSO and NAO by regressing out the NAO and ENSO signals from composite of detrended monthly anomalies of surface temperature field to isolate the impact of jet merging on them. The results suggest that despite the frequent alignment of -ZJI winter months with strong El Niño and negative NAO phases, anomalous temperature distributions persist during -ZJI winters although with slightly diminished intensity even after the removal of ENSO and NAO signals. Among this anomalous temperature distributions, the particularly noteworthy is the emergence of anomalous warming over the Arctic, a phenomenon  
335 previously obscured by the dominant NAO and ENSO signals. This anomalous warming trend could lead to decreased eddy activity (eddy fluxes and eddy kinetic energy) over these regions (Yuval and Kaspi, 2020; Chemke and Polvani, 2020). It also suggests a connection between -ZJI and Arctic Amplification, impacting atmospheric circulation patterns and potentially influencing extreme winter weather across midlatitudes.



In essence, during the merged-jet winters we see a distribution of surface temperature extremes along with a cumulation of tropical heating, over both the Atlantic and Pacific (mostly due to El Niño), together with anomalous warm Arctic and cold Eurasia which affects the midlatitude baroclinicity. This is something theorised in previous studies using idealised models that has shown to cause dynamical regime change from an eddy-driven jet to a mixed thermally–eddy-driven jet (Son and Lee, 2005; Lachmy and Harnik, 2014, 2016) but not documented well within the real world observations. Hence these results suggest that the Atlantic and African jet merging over the Atlantic Ocean shows the real world observations of a dynamical regime shift from an eddy-driven jet to a mixed thermally–eddy driven jet. Additionally, the development of warmer oceanic regions, particularly over the subtropical Atlantic and equatorial Pacific, could contribute to sustaining the merged Atlantic-African jet throughout the winter season thus affecting the extreme weather distribution over the Northern hemisphere. A potential feedback mechanism could be at play, where the warmer oceanic anomaly conditions over the tropical Pacific likely contribute to the initiation of jet merging, which leads to the warmer subtropical Atlantic anomalies that both drive and possibly maintain the merged jet state, which needs further study.

Secondly, our analysis of surface wind extremes revealed concentrated regions of strong winds over the subtropical Atlantic, Greenland, and the Eastern tropical Pacific during -ZJI winters, with a notable increase in frequency compared to typical -NAO winters. A strong wind activity over the tropical eastern Pacific continues to exist even after removing the NAO and ENSO signal which possibly indicate an anomalous overturning circulation that gives rise to the ongoing air flow into the Atlantic jet from the subtropical Pacific during jet-merging as suggested in (Harnik et al., 2014). Furthermore, our investigation into precipitation patterns demonstrated an increase in extreme precipitation over the Iberian Peninsula and western Greenland, while low precipitation over south-eastern Greenland coast during -ZJI winters, which was distinct from -NAO and El Niño winters. This highlights the significant impact of the merged jet event on regional precipitation distribution.

Finally, this study also shows the significant role of cyclones in driving extreme weather events during jet merging which acts as a crucial factor in their intensification, as well as in determining cyclone paths. By focusing on the -ZJI winter months, we have observed distinct patterns in cyclone behavior compared to typical -NAO winters, with cyclones exhibiting a pronounced southward and zonal shift due to merged jet formation. Notably, the -ZJI winter months also witness higher cyclone density over western Greenland, an uncommon occurrence in standard -NAO winters. This deviation is further highlighted by the stronger eddy kinetic energy observed during -ZJI winters, particularly over western Greenland and the Arctic Archipelago region. Overall, the analysis implies a noteworthy deviation from the conventional northeastward trajectory of cyclones during jet merging, with a significant proportion migrating towards the eastern Atlantic and extending across the Mediterranean while certain cyclones appear to move towards the western coast of Greenland, contributing to extreme anomalies observed in the region. These findings underscore the complex interplay between merged-jet dynamics over Atlantic and cyclonic activity, ultimately influencing regional weather patterns and extreme events. Given the possible increase in Arctic amplification and extreme El Niño in the future global warming scenario such persistent jet-merging due to dynamical regime shift and its associated extreme weather events can possibly occur more frequently. Hence further research in this area is crucial for enhancing our understanding of these phenomena and their potential implications for future climate scenarios.



*Code and data availability.* ERA5 data used in this study is freely available from the Copernicus Climate Change Service (C3S) Climate Data Store at <https://doi.org/10.24381/cds.f17050d7> (Hersbach et al., 2023a) and <https://doi.org/10.24381/cds.6860a573> (Hersbach et al., 375 2023b) , last access:16 March 2024. NAO index is available at: <https://www.cpc.ncep.noaa.gov/products/precip/CWlink/pna/nao.shtml> and Oceanic Nino Index (ONI) is available at: [https://origin.cpc.ncep.noaa.gov/products/analysis\\_monitoring/ensostuff/ONI\\_v5.php](https://origin.cpc.ncep.noaa.gov/products/analysis_monitoring/ensostuff/ONI_v5.php). Cyclone tracks found in ERA5 using the algorithm from Pinto et al. (2005) and all the additional codes used for this study are available upon request

*Author contributions.* SS, NH, and RC designed the analysis. SS carried out the analysis and drafted the first version of the manuscript with feedback from NH and RC. All authors contributed to discussions, structuring the analysis, and reviewing the paper.

380 *Competing interests.* At least one of the (co-)authors is a member of the editorial board of Weather and Climate Dynamics.

*Acknowledgements.* This research has been supported by funding from the European Union's Horizon 2020 research and innovation programme under Marie Skłodowska-Curie grant No.956396 (EDIPI project). The authors would like to thank Prof.Joaquim G. Pinto and his group at KIT, Germany for providing the cyclone track data. The authors would also like to thank Prof.Gabriele Messori, Aleksa Stankovic and Inovasita Alifdini for fruitful discussions during the early stages of the analysis, which helped to improve this work.



## 385 References

- Alexander, L. V., Uotila, P., and Nicholls, N.: Influence of sea surface temperature variability on global temperature and precipitation extremes, *Journal of Geophysical Research: Atmospheres*, 114, 2009.
- Amaya, D. J.: The Pacific meridional mode and ENSO: A review, *Current Climate Change Reports*, 5, 296–307, 2019.
- Arblaster, J. M. and Alexander, L. V.: The impact of the El Niño–Southern Oscillation on maximum temperature extremes, *Geophysical Research Letters*, 39, 2012.
- 390 Barnes, E. A. and Hartmann, D. L.: Dynamical feedbacks and the persistence of the NAO, *Journal of the Atmospheric Sciences*, 67, 851–865, 2010.
- Brönnimann, S., Luterbacher, J., Staehelin, J., Svendby, T., Hansen, G., and Svenjõe, T.: Extreme climate of the global troposphere and stratosphere in 1940–42 related to El Niño, *Nature*, 431, 971–974, 2004.
- 395 Cai, W., Borlace, S., Lengaigne, M., Van Rensch, P., Collins, M., Vecchi, G., Timmermann, A., Santoso, A., McPhaden, M. J., Wu, L., et al.: Increasing frequency of extreme El Niño events due to greenhouse warming, *Nature climate change*, 4, 111–116, 2014.
- Cattiaux, J., Vautard, R., Cassou, C., Yiou, P., Masson-Delmotte, V., and Codron, F.: Winter 2010 in Europe: A cold extreme in a warming climate, *Geophysical Research Letters*, 37, 2010.
- Chang, P., Zhang, L., Saravanan, R., Vimont, D. J., Chiang, J. C., Ji, L., Seidel, H., and Tippett, M. K.: Pacific meridional mode and El Niño—Southern oscillation, *Geophysical Research Letters*, 34, 2007.
- 400 Chemke, R. and Polvani, L. M.: Linking midlatitudes eddy heat flux trends and polar amplification, *npj Climate and Atmospheric Science*, 3, 8, 2020.
- Cohen, J., Screen, J. A., Furtado, J. C., Barlow, M., Whittleston, D., Coumou, D., Francis, J., Dethloff, K., Entekhabi, D., Overland, J., et al.: Recent Arctic amplification and extreme mid-latitude weather, *Nature geoscience*, 7, 627–637, 2014.
- 405 Cohen, J., Agel, L., Barlow, M., Garfinkel, C. I., and White, I.: Linking Arctic variability and change with extreme winter weather in the United States, *Science*, 373, 1116–1121, 2021.
- Donat, M., Peterson, T., Brunet, M., King, A., Almazroui, M., Kolli, R., Bouché, D., Al-Mulla, A. Y., Nour, A. Y., Aly, A. A., et al.: Changes in extreme temperature and precipitation in the Arab region: long-term trends and variability related to ENSO and NAO, *International Journal of Climatology*, 34, 581–592, 2014.
- 410 Drouard, M., Kornhuber, K., and Woollings, T.: Disentangling dynamic contributions to summer 2018 anomalous weather over Europe, *Geophysical Research Letters*, 46, 12 537–12 546, 2019.
- Eichelberger, S. J. and Hartmann, D. L.: Zonal jet structure and the leading mode of variability, *Journal of Climate*, 20, 5149–5163, 2007.
- Francis, J. A. and Vavrus, S. J.: Evidence linking Arctic amplification to extreme weather in mid-latitudes, *Geophysical research letters*, 39, 2012.
- 415 Harnik, N., Galanti, E., Martius, O., and Adam, O.: The anomalous merging of the African and North Atlantic jet streams during the Northern Hemisphere winter of 2010, *Journal of Climate*, 27, 7319–7334, 2014.
- Held, I. M.: Momentum transport by quasi-geostrophic eddies, *J. Atmos. Sci.*, 32, 1494–1497, 1975.
- Held, I. M. and Hou, A. Y.: Nonlinear axially symmetric circulations in a nearly inviscid atmosphere, *Journal of the Atmospheric Sciences*, 37, 515–533, 1980.
- 420 Hersbach, H., Bell, B., Berrisford, P., Biavati, G., Horányi, A., Muñoz Sabater, J., Nicolas, J., Peubey, C., Radu, R., Rozum, I., et al.: ERA5 monthly averaged data on single levels from 1940 to present [Dataset]. Copernicus Climate Change Service (C3S) Climate Data Store (CDS), 2023a.



- Hersbach, H., Bell, B., Berrisford, P., Biavati, G., Horányi, A., Muñoz Sabater, J., Nicolas, J., Peubey, C., Radu, R., Rozum, I., et al.: ERA5 monthly averaged data on single levels from 1940 to present [Dataset]. Copernicus Climate Change Service (C3S) Climate Data Store (CDS), 2023b.
- Holton, J. R.: An introduction to dynamic meteorology, Elsevier Academic Press Boston, 2007.
- Hurrell, J. W.: Decadal trends in the North Atlantic Oscillation: Regional temperatures and precipitation, *Science*, 269, 676–679, 1995.
- Jianping, L. and Wang, J. X.: A new North Atlantic Oscillation index and its variability, *Advances in Atmospheric Sciences*, 20, 661–676, 2003.
- 430 Kenyon, J. and Hegerl, G. C.: Influence of modes of climate variability on global precipitation extremes, *Journal of Climate*, 23, 6248–6262, 2010.
- Kim, B.-M., Son, S.-W., Min, S.-K., Jeong, J.-H., Kim, S.-J., Zhang, X., Shim, T., and Yoon, J.-H.: Weakening of the stratospheric polar vortex by Arctic sea-ice loss, *Nature communications*, 5, 4646, 2014.
- Kim, H.-k. and Lee, S.: The wave–zonal mean flow interaction in the Southern Hemisphere, *Journal of the atmospheric sciences*, 61, 1055–435 1067, 2004.
- Kim, J.-W., Yu, J.-Y., and Tian, B.: Overemphasized role of preceding strong El Niño in generating multi-year La Niña events, *Nature Communications*, 14, 6790, 2023.
- Kinnard, C., Zdanowicz, C. M., Fisher, D. A., Isaksson, E., de Vernal, A., and Thompson, L. G.: Reconstructed changes in Arctic sea ice over the past 1,450 years, *Nature*, 479, 509–512, 2011.
- 440 Lachmy, O. and Harnik, N.: The transition to a subtropical jet regime and its maintenance, *Journal of the Atmospheric Sciences*, 71, 1389–1409, 2014.
- Lachmy, O. and Harnik, N.: Wave and jet maintenance in different flow regimes, *Journal of the Atmospheric Sciences*, 73, 2465–2484, 2016.
- Lachmy, O. and Harnik, N.: Tropospheric jet variability in different flow regimes, *Quarterly Journal of the Royal Meteorological Society*, 146, 327–347, 2020.
- 445 Lee, S. and Kim, H.-k.: The dynamical relationship between subtropical and eddy-driven jets, *Journal of the atmospheric sciences*, 60, 1490–1503, 2003.
- Li, C. and Wettstein, J. J.: Thermally driven and eddy-driven jet variability in reanalysis, *Journal of Climate*, 25, 1587–1596, 2012.
- Lorenz, D. J. and Hartmann, D. L.: Eddy–zonal flow feedback in the Northern Hemisphere winter, *Journal of climate*, 16, 1212–1227, 2003.
- Lu, J., Chen, G., and Frierson, D. M.: The position of the midlatitude storm track and eddy-driven westerlies in aquaplanet AGCMs, *Journal of the Atmospheric Sciences*, 67, 3984–4000, 2010.
- 450 Michel, C. and Rivière, G.: Sensitivity of the position and variability of the eddy-driven jet to different SST profiles in an aquaplanet general circulation model, *Journal of the Atmospheric Sciences*, 71, 349–371, 2014.
- Moore, G. and Renfrew, I.: Cold European winters: interplay between the NAO and the East Atlantic mode, *Atmospheric Science Letters*, 13, 1–8, 2012.
- 455 Murray, R. J. and Simmonds, I.: A numerical scheme for tracking cyclone centres from digital data, *Australian meteorological magazine*, 39, 155–166, 1991.
- Neu, U., Akperov, M. G., Bellenbaum, N., Benestad, R., Blender, R., Caballero, R., Coccozza, A., Dacre, H. F., Feng, Y., Fraedrich, K., et al.: IMILAST: A community effort to intercompare extratropical cyclone detection and tracking algorithms, *Bulletin of the American Meteorological Society*, 94, 529–547, 2013.



- 460 O'Rourke, A. K. and Vallis, G. K.: Jet interaction and the influence of a minimum phase speed bound on the propagation of eddies, *Journal of the atmospheric sciences*, 70, 2614–2628, 2013.
- Panetta, R. L.: Zonal jets in wide baroclinically unstable regions: Persistence and scale selection, *Journal of the atmospheric sciences*, 50, 2073–2106, 1993.
- Peings, Y., Davini, P., and Magnusdottir, G.: Impact of Ural Blocking on Early Winter Climate Variability Under Different Barents-Kara Sea  
465 Ice Conditions, *Journal of Geophysical Research: Atmospheres*, 128, e2022JD036994, 2023.
- Pinto, J. G., Spanghel, T., Ulbrich, U., and Speth, P.: Sensitivities of a cyclone detection and tracking algorithm: individual tracks and climatology, *Meteorologische Zeitschrift*, 14, 823–838, 2005.
- Pinto, J. G., Zacharias, S., Fink, A. H., Leckebusch, G. C., and Ulbrich, U.: Factors contributing to the development of extreme North Atlantic cyclones and their relationship with the NAO, *Climate dynamics*, 32, 711–737, 2009.
- 470 Rantanen, M., Karpechko, A. Y., Lipponen, A., Nordling, K., Hyvärinen, O., Ruosteenoja, K., Vihma, T., and Laaksonen, A.: The Arctic has warmed nearly four times faster than the globe since 1979, *Communications Earth & Environment*, 3, 168, 2022.
- Rhines, P. B.: Waves and turbulence on a beta-plane, *Journal of Fluid Mechanics*, 69, 417–443, 1975.
- Ropelewski, C. F. and Halpert, M. S.: North American precipitation and temperature patterns associated with the El Niño/Southern Oscillation (ENSO), *Monthly Weather Review*, 114, 2352–2362, 1986.
- 475 Santos, J. A., Woollings, T., and Pinto, J. G.: Are the winters 2010 and 2012 archetypes exhibiting extreme opposite behavior of the North Atlantic jet stream?, *Monthly Weather Review*, 141, 3626–3640, 2013.
- Schneider, E. K.: Axially symmetric steady-state models of the basic state for instability and climate studies. Part II. Nonlinear calculations, *Journal of Atmospheric Sciences*, 34, 280–296, 1977.
- Schubert, S. D., Chang, Y., Suarez, M. J., and Pegion, P. J.: ENSO and wintertime extreme precipitation events over the contiguous United  
480 States, *Journal of Climate*, 21, 22–39, 2008.
- Screen, J. A. and Simmonds, I.: Amplified mid-latitude planetary waves favour particular regional weather extremes, *Nature Climate Change*, 4, 704–709, 2014.
- Seager, R., Kushnir, Y., Nakamura, J., Ting, M., and Naik, N.: Northern Hemisphere winter snow anomalies: ENSO, NAO and the winter of 2009/10, *Geophysical research letters*, 37, 2010.
- 485 Seager, R., Hoerling, M., Schubert, S., Wang, H., Lyon, B., Kumar, A., Nakamura, J., and Henderson, N.: Causes of the 2011–14 California drought, *Journal of Climate*, 28, 6997–7024, 2015.
- Son, S.-W. and Lee, S.: The response of westerly jets to thermal driving in a primitive equation model, *Journal of the atmospheric sciences*, 62, 3741–3757, 2005.
- Son, S.-W. and Lee, S.: Preferred modes of variability and their relationship with climate change, *Journal of climate*, 19, 2063–2075, 2006.
- 490 Thompson, D. W. and Wallace, J. M.: Regional climate impacts of the Northern Hemisphere annular mode, *Science*, 293, 85–89, 2001.
- Vicente-Serrano, S. M., Trigo, R. M., López-Moreno, J. I., Liberato, M. L., Lorenzo-Lacruz, J., Beguería, S., Morán-Tejeda, E., and El Ke-nawy, A.: Extreme winter precipitation in the Iberian Peninsula in 2010: anomalies, driving mechanisms and future projections, *Climate Research*, 46, 51–65, 2011.
- Wang, B., Luo, X., Yang, Y.-M., Sun, W., Cane, M. A., Cai, W., Yeh, S.-W., and Liu, J.: Historical change of El Niño properties sheds light  
495 on future changes of extreme El Niño, *Proceedings of the National Academy of Sciences*, 116, 22512–22517, 2019.
- Wang, C., Liu, H., and Lee, S.-K.: The record-breaking cold temperatures during the winter of 2009/2010 in the Northern Hemisphere, *Atmospheric Science Letters*, 11, 161–168, 2010.



- You, Y. and Furtado, J. C.: The role of South Pacific atmospheric variability in the development of different types of ENSO, *Geophysical Research Letters*, 44, 7438–7446, 2017.
- 500 Yuval, J. and Kaspi, Y.: Eddy activity response to global warming–like temperature changes, *Journal of Climate*, 33, 1381–1404, 2020.
- Zhang, H., Clement, A., and Di Nezio, P.: The South Pacific meridional mode: A mechanism for ENSO-like variability, *Journal of Climate*, 27, 769–783, 2014.